Vol 18 No 7, July 2009
1674-1056/2009/18(07)/2967-08

Chinese Physics B

© 2009 Chin. Phys. Soc.
and IOP Publishing Ltd

Effect of local structure on electron paramagnetic resonance spectra for trigonal $[Cr(H_2O)_6]^{3+}$ coordination complex in the sulfate alums series: a ligand field theory study*

Li Yan-Fang(李艳芳)[a], Kuang Xiao-Yu(邝小渝)[a)b)†], Gao Ming-Liang(高明亮)[a], Zhao Ya-Ru(赵亚儒)[a], and Wang Huai-Qian(王怀谦)[a]

[a] *Institute of Atomic and Molecular Physics, Sichuan University, Chengdu* 610065, *China*
[b] *International Centre for Materials Physics, Chinese Academy of Sciences, Shenyang* 110016, *China*

(Received 30 November 2008; revised manuscript received 17 December 2008)

A simple theoretical method is introduced for studying the interrelation between electronic and molecular structures. By diagonalizing the 120 × 120 complete energy matrices, the relationships between zero-field splitting (ZFS) parameter D and local distortion parameter $\Delta\theta$ for Cr^{3+} ions doped, separately, in α- and β- alums are investigated. Our results indicate that there exists an approximately linear relationship between D and $\Delta\theta$ in a temperature range 4.2–297 K and the signs of D and $\Delta\theta$ are opposite to each other. Moreover, in order to understand the contribution of spin–orbit coupling coefficient ζ to ZFS parameter D, the relation between D and ζ is also discussed.

Keywords: complete energy matrices, electron paramagnetic resonance (EPR) spectra, local structure

PACC: 7170C, 7630, 7630F

1. Introduction

The alums belong to a well-known class of isostructural double salts described with a general formula $M^{I}M^{III}(RO_4)_2{\cdot}12H_2O$, where M^{I} represents a univalent cation such as Na^+, K^+, Rb^+, Cs^+, Tl^+, and NH_4^+, M^{III} denotes a trivalent mental ion, such as Al^{3+}, Ga^{3+}, In^{3+}, Ti^{3+}, V^{3+}, Cr^{3+}, Mn^{3+}, Fe^{3+} and Mo^{3+}, and R refers to S or Se.[1−4] The structures of these compounds are characterized by the same cubic space group $Pa\overline{3}(T_h^6)$ with four formula units per unit cell ($Z = 4$). Since Lipson[5] found that the alums could be decomposed into three different structural types designated as α-, β- and γ-, the alums have attracted much attention.[6−9] During the last several decades, many experiments on, such as x-ray diffraction,[10] vibrational spectra[11] and HFEPR[12] have been performed to study the hyperfine structure of alums. Recently, Beattie *et al*[13] have successfully proved that the difference between the α- and the β- categories may be elucidated by the geometry of six water molecules around a univalent cation. In α-alums there exists a trigonal antiprism along the three-fold axis, and the H_2O-M^{I}-H_2O angle lies in a range of 64.6–66.5°, while in β-alums the corresponding value is in a 60.0–60.2° range. The distinguishing feature of γ-alums is the orientation of the sulfate (selenate) group. The schematic drawing of α- and β-alums has been reported[3] as shown in Fig.1.

The advantage of the alum structure is accommodating a wide range of trivalent cations with little change of the lattice. This makes it very suitable as a host lattice to study the properties of crystal doped with transition metal ions.[7,9,14,15] Among the varieties of experimental techniques, electron paramagnetic resonance (EPR) is regarded as an effective tool to study the microstructure and the local environment around a substitution magnetic ion site in crystals.[16−24] For instance, the interrelation between electronic and molecular structures is well illustrated by Tregenna-Piggott *et al*[25] by using EPR parameters for the $[V(H_2O)_6]^{3+}$ coordination complex in various alums. Tregenna-Piggott *et al* pointed out that the electronic structure of the complex depends strongly on the mode of coordination of water molecules to the V^{3+} ion, which was revealed by single-crystal neutron

*Project supported by the National Natural Science Foundation of China (Grant No 10774103) and the Doctoral Education Fund of Education Ministry of China (Grant No 20050610011).
†E-mail: scu_kuang@163.com

and x-ray diffraction measurements. Subsequently, Krivokapič *et al*[6] studied high-field multifrequency EPR spectra of Mn^{3+} ion doped in the CsGa sulfate alum, and they presented the first observation and interpretation of the anisotropic hyperfine interaction in the $[Mn(H_2O)_6]^{3+}$ coordination complex. In addition, a phase transition from cubic ($Pa\bar{3}$) to orthorhombic ($Pbca$) at 156 K was also observed in alums. Especially, Manoogian and Leclerc[26] carried out a systematical study on the zero-field splitting (ZFS) parameter D as a function of temperature for $[Cr(H_2O)_6]^{3+}$ magnetic complexes in alums. From the experimental results, Manoogian and Leclerc found an interesting phenomenon that the magnitude of D decreases with temperature decreasing for all alums, $D > 0$ for α-alums and $D < 0$ for β-alums.

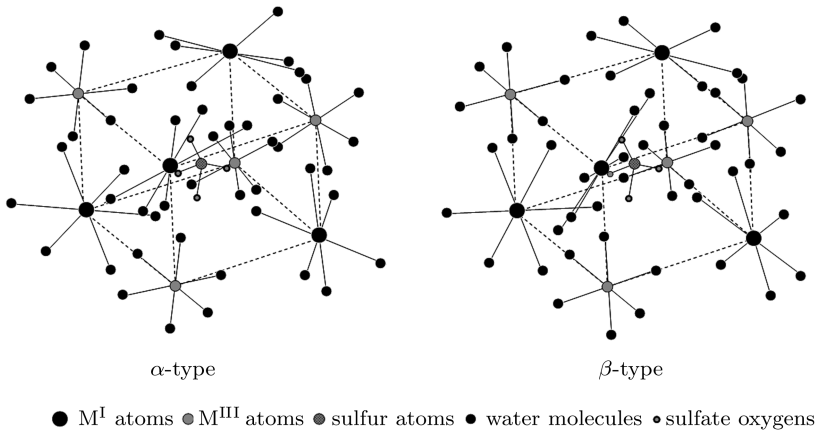


Fig.1. Schematics of the crystal structure of α- and β-alums.

From the extensive EPR experiments much important information about the local structure of the magnetic impurity centre is obtained, thereby forming a useful starting point for understanding the interrelation between electronic and molecular structures of transition metal ions in alums. However, the systematical theoretical investigation of the local structures around impurities in different alums has been little performed. In the present paper, different local structures of $[Cr(H_2O)_6]^{3+}$ octahedron in α- and β-sulfate alums are determined, separately, and the influence of the local distortion parameter $\Delta\theta$ on ZFS parameter D is studied in a temperature range 4.2–297 K. Meanwhile, the relationship between ZFS parameter D and spin–orbit coupling coefficient ζ is also studied.

2. Method

2.1. Complete energy matrices for the d^3 configuration ion in the trigonal ligand-field

The method of diagonalizing the complete energy matrices has been proved to be a powerful tool to study the interrelation between electronic and molecular structures. For the d^3 configuration ion in a trigonal ligand-field, the corresponding perturbation Hamiltonian can be expressed as

$$\hat{H} = \hat{H}_{\rm ee} + \hat{H}_{\rm SO} + \hat{H}_{\rm LF} + \hat{H}_{\rm ZEE} = \sum_{i<j} e^2/r_{i,j} + \zeta \sum_i l_i{\cdot}s_i + \sum_i V_i + \sum_i \mu_{\rm B}(k\boldsymbol{l}_i + g_{\rm e}\boldsymbol{s}_i)\cdot\boldsymbol{H}, \tag{1}$$

where $\hat{H}_{\rm ee}$, $\hat{H}_{\rm SO}$, $\hat{H}_{\rm LF}$ and $\hat{H}_{\rm ZEE}$ are, respectively, electron–electron repulsion interaction, spin–orbit coupling interaction, ligand–field interaction and Zeeman interaction; k is the orbit reduction factor; V_i is the ligand-field potential.

With the use of $|L, S, M_{\rm L}, M_{\rm S}\rangle$ basic functions, the 120×120 complete energy matrices of the Hamiltonian including two directions of the external magnetic field have been established by using Slater's method.[27,28] The matrix elements are functions of Racah parameters B and C, spin–orbit coupling coefficient ζ and ligand-field parameters B_{20}, B_{40}, $B_{43}^{\rm c}$ and $B_{43}^{\rm s}$. Generally, the z-axis is chosen to be along the C_3 axis and the x-axis is set

to be consistent with the projection of one of the impurity-ligand bonds in the x–y plane. Then parameter B^{s}_{43} will vanish and the other terms can be written as[29]

$$B_{20} = \frac{1}{2}\sum_{\tau}\frac{A_2}{R^3_\tau}(3\cos^2\theta_\tau - 1),$$
$$B_{40} = \frac{1}{8}\sum_{\tau}\frac{A_4}{R^5_\tau}(35\cos^4\theta_\tau - 30\cos^2\theta_\tau + 3),$$
$$B^{c}_{43} = \frac{\sqrt{35}}{4}\sum_{\tau}\frac{A_4}{R^5_\tau}\sin^3\theta_\tau\cos\theta_\tau, \quad (2)$$

where

$$A_2 = -eq_\tau\langle r^2\rangle, \quad A_4 = -eq_\tau\langle r^4\rangle,$$

and

$$A_2/A_4 = \langle r^2\rangle/\langle r^4\rangle. \quad (3)$$

We use R_τ and θ_τ to represent the impurity-ligand distance and the corresponding angle between the impurity-ligand bond and the C_3 axis, respectively.

The ratio of $\langle r^2\rangle/\langle r^4\rangle = 0.151227$ is obtained from the parametric radial wavefunction.[30] For a $[Cr(H_2O)_6]^{3+}$ octahedron, A_4 is almost a constant and its value can be determined from the optical spectra and the Cr–H_2O bond length of the $KCr(SO_4)_2{\cdot}12H_2O$.[1,31] In this way, we acquire $A_4 = 33.01$ a.u. and $A_2 = 4.99$ a.u., which will be adopted in the following calculation. In order to reduce the number of adjustable parameters and reflect the effects of covalence, we take average covalence factor N and use the following relations:

$$B = N^4B_0, \quad C = N^4C_0,$$

and

$$\zeta = N^2\zeta_0 \quad (4)$$

where $B_0 = 1030$ cm^{-1}, $C_0 = 3850$ cm^{-1}, and $\zeta_0 = 273$ cm^{-1} are the free Cr^{3+} ion parameters.[32]

2.2. EPR parameters for the d^3 configuration ion

The EPR spectra of the d^3 configuration ion Cr^{3+} in a trigonal ligand-field can be analysed by employing the spin Hamiltonian[33]

$$\hat{H}_S = g_\parallel\mu_B H_z S_z + g_\perp\mu_B(H_xS_x + H_yS_y) + D[S_z^2 - (1/3)S(S+1)], \quad (5)$$

where D is the ZFS parameter. For the total spin $S = 3/2$, the eigenvalues of the spin Hamiltonian depend on the direction of the external magnetic field. For $H_\parallel(H_z)$, the splitting energy levels are

$$E_1 = D + \frac{3}{2}g_\parallel\mu_B H_\parallel,$$
$$E_2 = -D + \frac{1}{2}g_\parallel\mu_B H_\parallel,$$
$$E_3 = -D - \frac{1}{2}g_\parallel\mu_B H_\parallel,$$

and

$$E_4 = D - \frac{3}{2}g_\parallel\mu_B H_\parallel, \quad (6)$$

while for $H_\perp(H_x$ or $H_y)$, they are

$$E_1 = -\frac{1}{2}g_\perp\mu_B H_\perp + \sqrt{g_\perp^2\mu_B^2H_\perp^2 + D^2 + Dg_\perp\mu_B H_\perp},$$
$$E_2 = -\frac{1}{2}g_\perp\mu_B H_\perp - \sqrt{g_\perp^2\mu_B^2H_\perp^2 + D^2 + Dg_\perp\mu_B H_\perp},$$
$$E_3 = \frac{1}{2}g_\perp\mu_B H_\perp + \sqrt{g_\perp^2\mu_B^2H_\perp^2 + D^2 - Dg_\perp\mu_B H_\perp},$$
$$E_4 = \frac{1}{2}g_\perp\mu_B H_\perp - \sqrt{g_\perp^2\mu_B^2H_\perp^2 + D^2 - Dg_\perp\mu_B H_\perp}. \quad (7)$$

It is known that the ground-state electronic term for the free Cr^{3+} ion is $^4F_{3/2}$. An octahedral ligand-field yields the ground state $^4A_2$, which is split by the additional trigonal ligand-field into two Kramers doublets with quantum numbers $M_s = \pm 3/2$ and $M_s = \pm 1/2$, separately. In the special case of the zero magnetic field, the ZFS energy ΔE between the two Kramers levels can be expressed as a function of parameter D

$$\Delta E = E(\pm 3/2) - E(\pm 1/2) = 2D. \quad (8)$$

Based on the above theoretical formulae and complete energy matrices, the interrelation between electronic and molecular structures can be established by analysing the EPR and optical spectra.

3. Calculation and discussion

3.1. Calculation of the local structure for the Cr^{3+} ion doped in sulfate alums

As already mentioned, all alums belong to the same space group and their unit cell parameters are close to each other. Their slight differences in atomic arrangement enable three types of alum structures to be determined (α-, β-, γ-). In each case there is a nearly regular octahedron of water molecules

surrounding a trivalent ion. In our present work, the alums $M^{I}M^{III}(SO_4)_2{\cdot}12H_2O$ (M^{I} = Rb^+, Tl^+, NH_4^+; M^{III} = Al^{3+}, Ga^{3+}) are of α-alum while alums $CsM^{III}(SO_4)_2{\cdot}12H_2O$ (M^{III} = Al^{3+}, Ga^{3+}) are of β-alum. When it is doped into these sulfate alums, the Cr^{3+} ion will occupy the site of the host M^{III} ion, and the local structure around the Cr^{3+} centre will display a trigonal distortion along the C_3 axis, owing to the ionic radius and mass of the Cr^{3+} ion being different from those of the M^{III} ion. In order to describe the local structure of the $[Cr(H_2O)_6]^{3+}$ octahedron in sulfate alums, we introduce two parameters R and θ, which denote the Cr^{3+}–H_2O bond length and the angle between the Cr^{3+}–H_2O bond and the C_3 axis, respectively, as plotted in Fig.2.

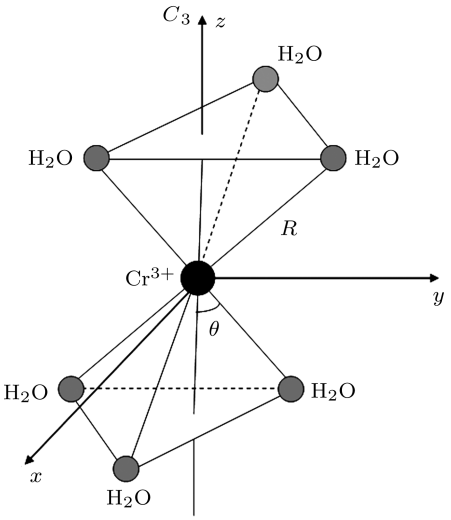


Fig.2. The microstructure for the Cr^{3+} ion doped in alums, where R is the Cr^{3+}–H_2O bond length and θ is the angle between the Cr^{3+}–H_2O bond and the C_3 axis.

For the local structure parameter R, its value can be determined by the optical spectra. However, the optical spectra of the Cr^{3+} ion doped in the above sulfate alums have not been reported. Many experimental results show that the $[Cr(H_2O)_6]^{3+}$ coordination complexes have similar energies,[31–34] so it is a reasonable approximation to apply the optical spectra of $AlCl_3{\cdot}6H_2O{:}Cr^{3+}$ system to our calculation. In this case we obtain $R = 1.960$ Å (297 K), 1.959 Å (195 K), 1.955 Å (77 K) and 1.954 Å (4.2 K) by simulating the optical spectrum energy ($^4A_2 \rightarrow {}^4T_2$) at different temperatures. Meanwhile, $N = 0.922$ (297 K), 0.926 (195 K), 0.923 (77 K) and 0.925 (4.2 K) can also be obtained. The local structure parameter θ for the Cr^{3+} ion doped in different sulfate alums can be expressed as:

$$\theta = \theta_{\rm oh} + \Delta\theta, \tag{9}$$

where $\theta_{\rm oh}$ denotes the bond angle between the M^{III}–H_2O bond and the C_3 axis in cubic symmetry ($\theta_{\rm oh} = \cos^{-1}(1/\sqrt{3}) \approx 54.7356°$), and $\Delta\theta$ represents the distortion of the bond angle. According to the previous studies,[17,22,35–37] the EPR parameters (D, $g_\parallel$, $g_\perp$) are more sensitive to the change of bond angle than that of bond length. Thus, with the above bond length at a corresponding temperature fixed, we investigate local distortion parameter $\Delta\theta$ in various sulfate alums by fitting the calculated EPR parameters to the observed ones. In order to obtain the calculations of the g-factors, the orbit reduction factor k is adjusted slightly according to the formula $k \approx N^2$. By diagonalizing the complete energy matrices, the optical spectra and EPR parameters of $[Cr(H_2O)_6]^{3+}$ coordination complex in various sulfate alums are calculated using the above parameters. The comparisons between the theoretical values and the experimental data are listed in Tables 1–3.

Table 1. Calculated optical spectrum energies ($^4A_2 \rightarrow {}^4T_2$) for Cr^{3+} ion doped in various alums at 297, 195, 77 and 4.2 K in units of cm^{-1}.

compounds	297 K		195 K		77 K		4.2 K	
CsGa alum	17275	17369	17307	17397	17488	17576	17500	17587
CsAl alum	17271	17371	17303	17399	17483	17578	17496	17589
RbGa alum	17301	17411	17339	17425	17523	17594	17535	17604
RbAl alum	17307	17398	17346	17409	17531	17578	17542	17589
TlGa alum	17299	17414	17339	17424	17527	17586	17538	17598
TlAl alum	17307	17398	17348	17408	17533	17575	–	–
NH_4Ga alum	17308	17397	17350	17403	–	–	–	–
NH_4Al alum	17316	17380	17357	17388	–	–	–	–
expt.[34]	17240	17420	17240	17480	17540	17540	17540	17540

Table 2. Values of ZFS parameter D for the Cr^{3+} ion doped in various alums each as a function of parameter $\Delta\ \theta$ at 297, 195, 77 and 4.2 K, separately.

	297 K		195 K		77 K		4.2 K	
compounds	$\Delta\theta/(°)$	D/cm^{-1}	$\Delta\theta/(°)$	D/cm^{-1}	$\Delta\theta/(°)$	D/cm^{-1}	$\Delta\theta/(°)$	D/cm^{-1}
CsGa alum	0.190	–0.0719	0.183	–0.0697	0.177	–0.0667	0.175	–0.0660
expt.[26]		–0.0719		–0.0697		–0.0667		–0.0660
CsAl alum	0.201	–0.0762	0.196	–0.0744	0.192	–0.0723	0.189	–0.0715
expt.[26]		–0.0762		–0.0744		–0.0723		–0.0715
RbGa alum	–0.215	0.0824	–0.168	0.0645	–0.138	0.0525	–0.136	0.0518
expt.[26]		0.0824		0.0645		0.0525		0.0518
RbAl alum	–0.178	0.0681	–0.124	0.0474	–0.092	0.0348	–0.092	0.0349
expt.[26]		0.0681		0.0474		0.0348		0.0349
TlGa alum	–0.225	0.0862	–0.168	0.0643	–0.117	0.0444	–0.116	0.0442
expt.[26]		0.0862		0.0643		0.0444		0.0442
TlAl alum	–0.179	0.0683	–0.119	0.0457	–0.084	0.0320		
expt.[26]		0.0683		0.0457		0.0320	–	–
NH_4Ga alum	–0.174	0.0665	–0.106	0.0404				
expt.[26]		0.0665		0.0404	–	–	–	–
NH_4Al alum	–0.127	0.0485	–0.061	0.0232				
expt.[26]		0.0485		0.0232	–	–	–	–

Table 3. Calculated values of g-factors ($g_\parallel$, $g_\perp$) for Cr^{3+} ion doped in various alums and orbit reduction factor k. The experimental g-factors of all alums are 1.975±0.005 at 297, 195, 77 and 4.2 K that are cited from Ref.[26].

	297 K			195 K			77 K			4.2 K		
compounds	k	$g_\parallel$	$g_\perp$	k	$g_\parallel$	$g_\perp$	k	$g_\parallel$	$g_\perp$	k	$g_\parallel$	$g_\perp$
CsGa alum	0.746	1.9747	1.9753	0.742	1.9747	1.9752	0.756	1.9747	1.9752	0.752	1.9747	1.9752
CsAl alum	0.746	1.9747	1.9753	0.742	1.9747	1.9753	0.756	1.9747	1.9752	0.752	1.9747	1.9752
RbGa alum	0.756	1.9752	1.9745	0.749	1.9752	1.9747	0.759	1.9752	1.9748	0.756	1.9752	1.9748
RbAl alum	0.753	1.9752	1.9747	0.746	1.9752	1.9748	0.758	1.9752	1.9749	0.754	1.9752	1.9749
TlGa alum	0.756	1.9752	1.9745	0.749	1.9752	1.9747	0.759	1.9752	1.9748	0.755	1.9752	1.9748
TlAl alum	0.753	1.9752	1.9747	0.746	1.9752	1.9748	0.757	1.9752	1.9749	–	–	–
NH_4Ga alum	0.753	1.9752	1.9747	0.745	1.9752	1.9749	–	–	–	–	–	–
NH_4Al alum	0.751	1.9752	1.9748	0.743	1.9752	1.9750	–	–	–	–	–	–

From Tables 1–3, we can see that the experimental results can be satisfactorily simulated by the corresponding distortion parameters at each temperature. However, no measurement has been performed at some temperatures for TlAl, NH_4Ga and NH_4Al alums. The reason is that the linewidth of the EPR spectrum becomes excessively broad at 4.2 K for the TlAl alum and the NH_4 alums undergo a phase transition at low temperatures.[26] It must be pointed out that, owing to the influence of the H^+ ions, the calculated values of local structure parameters R and θ represent the equivalent position of the effective charge of the H_2O molecule rather than that of the O^{2+} ion.

3.2. Relationship between ZFS parameter D and local distortion parameter $\Delta\theta$

At each temperature, we calculate the values of local distortion parameter $\Delta\theta$ in various sulfate alums by fitting the calculated EPR parameters to the observed ones, with the corresponding bond length fixed, as mentioned above. In order to investigate the dependence of the ZFS parameter D on local distortion parameter $\Delta\theta$, the relationship between D and $\Delta\theta$ at each temperature is plotted in Fig.3. At each temperature, it can be seen that the ZFS parameter D varies sensitively with the change of parameter $\Delta\theta$ for Cr^{3+} ion doped in various sulfate alums, and there exists an approximately linear relationship between parameters D and $\Delta\theta$. For

different temperatures, we have found that the corresponding curves for D versus $\Delta\theta$ are different. However, it is worth noting that the slopes of curves for D versus $\Delta\theta$ at different temperatures are almost the same, whose value is –0.38. This means that the dependences of the ZFS parameter D on local distortion parameter $\Delta\theta$ are almost the same in the temperature range 4.2–297 K.

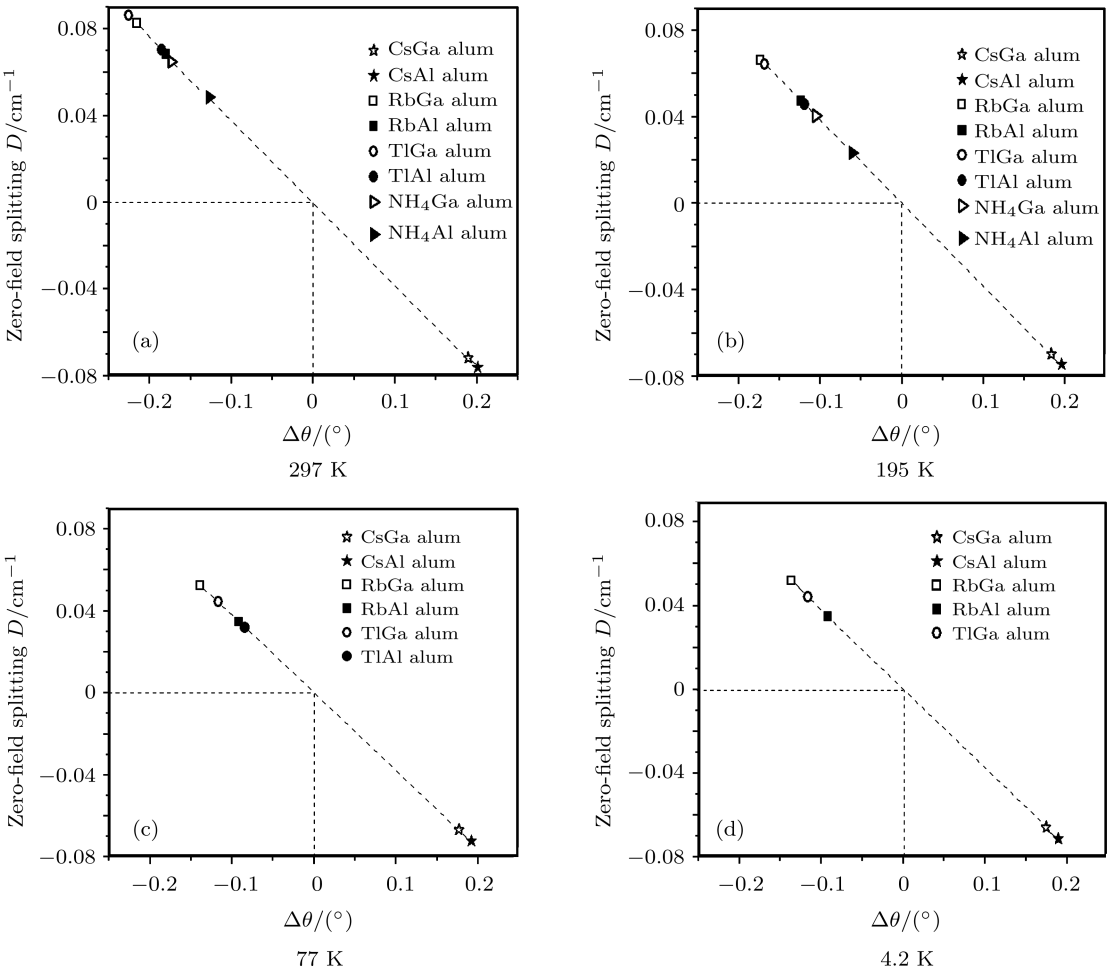


Fig.3. Effects of local distortion parameter $\Delta\theta$ on the ZFS parameter D for Cr^{3+} ion doped in various alums at 297 (a), 195 (b), 77 (c) and 4.2 K (d).

From Fig.3 we can clearly see that the signs of parameters D and $\Delta\theta$ are opposite to each other. The positive value of ZFS parameter D is related to an elongated distortion along the C_3 axis ($\theta < \theta_{\mathrm{oh}}$); while the negative sign of ZFS parameter D corresponds to a compressed distortion for the octahedron ($\theta > \theta_{\mathrm{oh}}$). With regard to the trigonal Cr^{3+} centres in different types of alums, the results show that in the local structure of the $[Cr(H_2O)_6]^{3+}$ octahedron there exist an elongated distortion for α-alums (M^{I} = Rb, NH_4, Tl) and a compressed distortion for β-alums (M^{I} = Cs) in the temperature range 4.2–297 K. Different trigonal distortions between α- and β-alums may be caused by the difference in coordination of M^{I} cation between α-alums (6-fold) and β-alums (12-fold).[3] It is worth pointing out that our theoretical results about the local structures of α- and β-alums can provide a powerful guideline for the further study of classifying the alums, because the best criterion about the alum classification is still in controversy.

Besides, we can see that the absolute value of ZFS parameter D reflects the magnitude of the distortion relative to the regular octahedron. For all alums, their magnitudes of ZFS parameter D decrease with temperature decreasing, which can be ascribed to the fact that there exist a decreasing elongation for α-alums and a decreasing compression for β-alums.

In addition, at each temperature, the magnitude of the distortion of Ga alum is found to be greater than that of the corresponding Al alum for α-alums but smaller for β-alums (see Table 2).

3.3. Influence of spin–orbit coupling coefficient ζ on ZFS parameter D

By using the corresponding parameters above and adjusting the spin–orbit coupling coefficient ζ, the values of ZFS parameter D are determined for different values of ζ based on the complete energy matrices. The curves for D versus ζ at 297 K are plotted for several different alums in Fig.4. Apparently, the spin–orbit coupling coefficient ζ has an important effect on

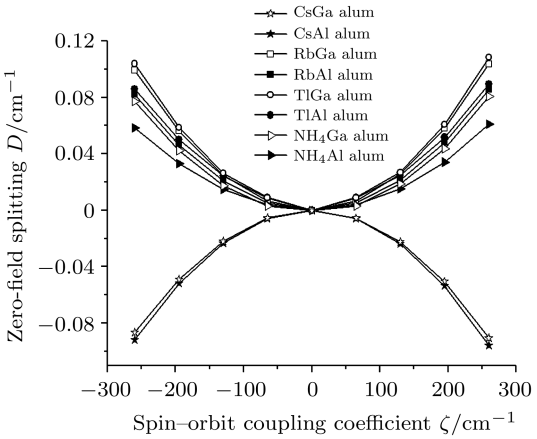


Fig.4. Relationship between ZFS parameter D and spin–orbit coupling coefficient ζ for Cr^{3+} ion doped in several different alums at 297 K.

ZFS parameter D, and in each system there exists an approximately quadratic relationship between D and ζ.

As suggested in Fig.4, there is a sequence of the magnitudes of $\partial D/\partial\zeta$, that is, TlGa alum > RbGa alum > CsAl alum > CsGa alum > TlAl alum > RbAl alum > NH_4Ga alum > NH_4Al alum. The difference in magnitude of $\partial D/\partial\zeta$ may be ascribed to the different local structures for Cr^{3+} ion doped in the alums.

4. Conclusions

The interrelations between EPR parameters and the local structure of $[Cr(H_2O)_6]^{3+}$ coordination complexes in various alums are analysed by diagonalizing the 120×120 complete energy matrices for the d^3 configuration ion in a trigonal ligand-field.

The relationship between ZFS parameter D and local distortion parameter $\Delta\theta$ is studied. The results reveal that the parameter $\Delta\theta$ has an important effect on ZFS parameter D and there exists an approximately linear relationship between D and $\Delta\theta$ in a temperature range 4.2–297 K. Meanwhile, we find that the positive value of the ZFS parameter D is related to an elongated distortion while the negative value corresponds to a compressed distortion.

The different local distortions around Cr^{3+} centres in α- and β-alums are found separately. The calculated results indicate that the local structure of the $[Cr(H_2O)_6]^{3+}$ coordination complex has an elongated distortion in α-alum and a compressed distortion in the β-alum. This result is of significance in deeply understanding the classification of alums. Of course, our theoretical results need to be verified by further experiments.

Considering the contribution of spin–orbit coupling coefficient ζ to ZFS parameter D, we can see that there is an approximately quadratic relationship between them.

References

[1] Nyburg S C, Steed J W, Aleksovska S and Petrusevski V M 2000 *Acta Cryst.* B **56** 204

[2] Rempfer N, Lerner H W and Bolte M 2004 *Acta Cryst.* E **60** i80

[3] Petruševski V M and Šoptrajanov B 2002 *Bull. Chem. Technol. Macedonia* **21** 103

[4] Beattie J K and Best S P 1997 *Coord. Chem. Rev.* **166** 391

[5] Lipson H 1935 *Proc. Roy. Soc.* A **151** 347

[6] Krivokapič I, Noble C, Klitgaard S, Tregenna-Piggott P, Weihe H and Barra A L 2005 *Angew. Chem. Int. Ed.* **44** 3613

[7] Krzystek J, Ozarowski A and Telser J 2006 *Coord. Chem. Rev.* **250** 2308

[8] Tregenna-Piggott P L W, Best S P, O'Brien M C M, Knight K S, Forsyth J B and Pilbrow J R 1997 *J. Am. Chem. Soc.* **119** 3324

[9] Armstrong R S, Berry A J, Cole B D and Nugent K W 1997 *J. Chem. Soc. Dalton Trans.* 363

[10] Beattie J K, Best S P, Favero P D, Skelton B W, Sobolev A N and White A H 1996 *J. Chem. Soc. Dalton Trans.* 1481

[11] Petruševski V M, Ivanovski V, Šoptrajanov B and Zugik M 2001 *J. Mol. Struct.* **563–564** 329

[12] Tregenna-Piggott P L W, Weihe H and Barra A L 2003 *Inorg. Chem.* **42** 8504

[13] Beattie J K, Best S P, Skelton B W and White A H 1981 *J. Chem. Soc. Dalton Trans.* 2105
[14] Tregenna-Piggott P L W, Noble C J and Pilbrow J R 2000 *J. Chem. Phys.* **113** 3289
[15] Tregenna-Piggott P L W, Best S P, Güdel H U, Weihe H and Wilson C C 1999 *J. Solid State Chem.* **145** 460
[16] Zhao J J, Xing R, Lu Y, Haosibayar, Zhao M Y, Jin X, Zheng L, Ning W, Sun Y and Cheng Z H 2008 *Chin. Phys.* B **17** 2721
[17] Kuang X Y, Mao A J and Wang H 2008 *J. Phys. Chem.* A **112** 737
[18] Lu C, Kuang X Y, Tan X M and Yang X 2007 *J. Phys. Chem.* A **111** 2783
[19] Kuang X Y and Lu C 2006 *J. Phys. Chem.* A **110** 11353
[20] Hou B H, Zheng Y G, Shao M, Liu F Y and Fan Z D 2005 *Chin. Phys.* **14** 1453
[21] Die D, Kuang X Y, Guo J J, Wang H and Zhou K W 2005 *Phys. Rev.* B **72** 073101
[22] Wang H Q, Kuang X Y and Li H F 2007 *Chem. Phys. Lett.* **444** 101
[23] Li F Z and Li Z M 2002 *Chin. Phys.* **11** 940
[24] Li F Z and Zhou Y Y 1998 *Acta Phys. Sin.* **47** 472 (in Chinese)
[25] Tregenna-Piggott P L W, Spichiger D, Carver G and Frey B 2004 *Inorg. Chem.* **43** 8049
[26] Manoogian A and Leclerc A 1975 *J. Chem. Phys.* **63** 4450
[27] Kuang X Y 1987 *Phys. Rev.* B **36** 712
[28] Kuang X Y 1987 *Phys. Rev.* B **36** 797
[29] Newman D J and Urban W 1975 *Adv. Phys.* **24** 793
[30] Zhao M G, Xu J A, Bai G R and Xie H S 1983 *Phys. Rev.* B **27** 1516
[31] Kesavamoorthy R and Krishnaswamy R 1981 *Phys. Status Solidi* (b) **108** 307
[32] Griffith J S 1964 *The Theory of Transition-metal Ions* (London: Cambridge University Press) p376
[33] Abragam A and Bleany B 1970 *Electron Paramagnetic Resonance of Transition Ions* (London: Oxford University Press) p430
[34] Carlin R L and Walker I M 1967 *J. Chem. Phys.* **46** 3921
[35] Feng W L, Zheng W C, Wu X X and Liu H G 2007 *Physica* B **387** 52
[36] Krupska A and Krupski M 2003 *Acta Phys. Pol.* A **103** 453
[37] Li Z M and Shuen W L 1996 *Physica* B **222** 238